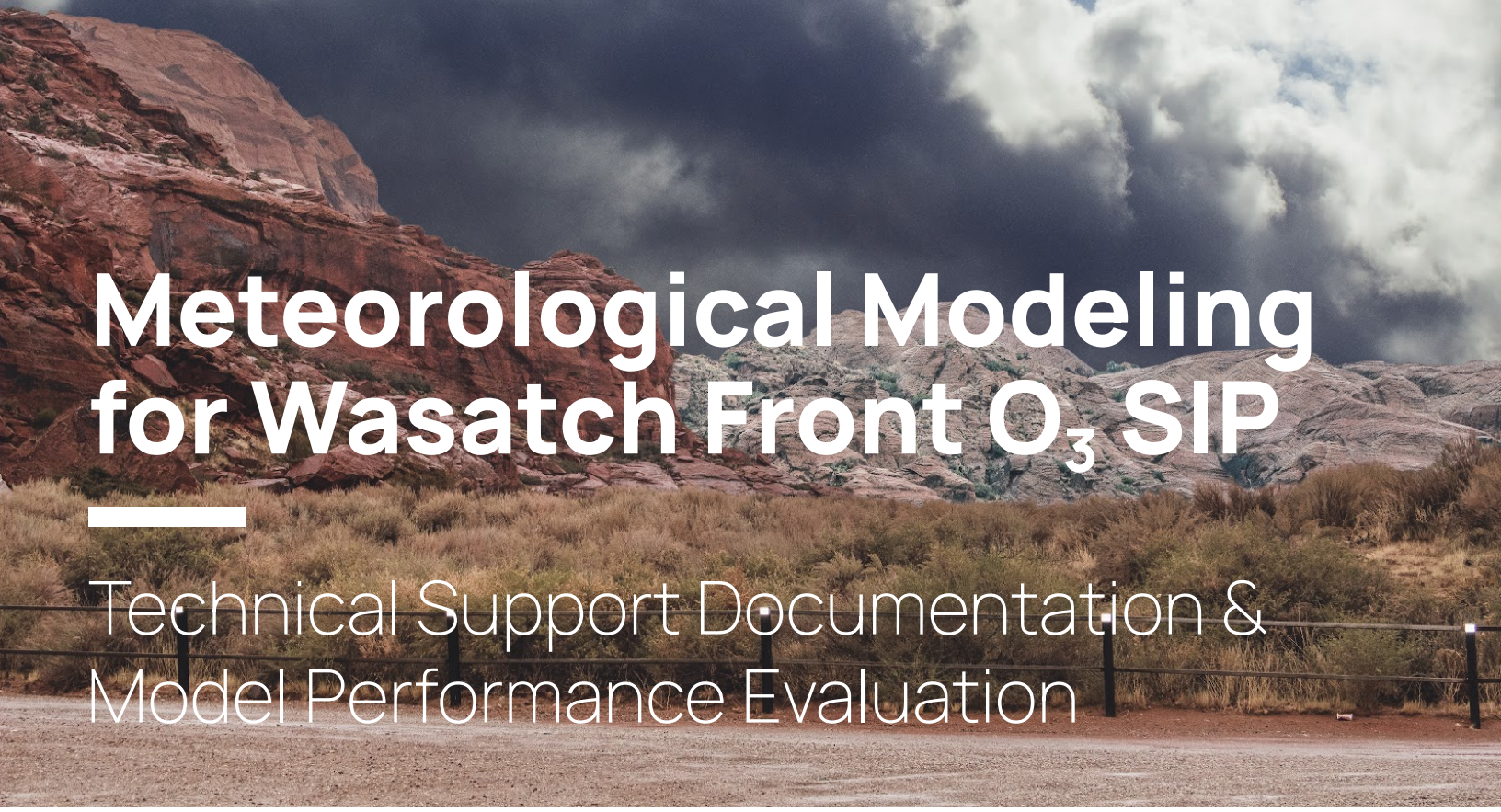

Meteorological Modeling for Wasatch Front O_3 SIP

Technical Support Documentation & Model Performance Evaluation

PREPARED BY Rachel Edie, PhD., Technical Analysis Section

UTAH DEPARTMENT of ENVIRONMENTAL QUALITY

Table of Contents

Table of Contents

Summary

1. WRF

1.1 WRF platform and preprocessor characteristics

Figure 1.1 - Extent of the 12, 4, and 1.33 km WRF modeling domains

1.1.1 Modeling domains and vertical layers

Table 1.1 - Brief summary of vertical levels and level thicknesses

1.1.2 Atmospheric data selection (IC/BC)

1.1.3 Geographic data selection

1.1.4 Adjustments to the Great Salt Lake Extent

Figure 1.2 - Great Salt Lake extent and depth before (left panel) and after (middle panel) adjusting the WRF geogrid files to reflect the GSL levels in mid-July of 2017 (right panel).

1.1.5 Additional Pre-Processor Selections

1.1.6 WRF Parameters Summary Table

Table 1.2 - WRF model grid configurations, land use, and initial/boundary conditions.

1.2 WRF Model Configuration

1.2.1 Model run length and outputs

1.2.2 Physics options

Table 1.3 - Physics options for WRF namelist

1.2.3 Dynamics options

1.2.4 Data assimilation & Nudging

1.2.5 Additional output variables

2. Model Performance Evaluation

2.1 Observational Datasets

Figure 2.1 - METAR sites along the Wasatch Front. KOGD, KHIF, KSLC, and KU42 are a part of the ozone NAA.

2.2 Spatial Surface Analysis (12 km)

Figure 2.2 - RMSE of 2m temperature, mixing ratio, and wind speed for the 12 km domain (D01).

Section 2.3 PRISM analysis

Figure 2.3 - July total WRF and PRISM estimated precipitation (mm) over the 12 km domain

Figure 2.4 - 4 km precipitation anomaly plots (WRF-PRISM) for June 15-30, 2017 (left) and July 2017 (right).

Figure 2.5. Precipitation anomaly plots (WRF-PRISM) for the 1.33 km modeling domain.

2.4 Time series analysis

Figure 2.2 - Time series of WRF simulation for METAR sites within the NAA.

Figure 2.3 - Time series of modeled vs observations at KSLC for D01 and D02

Figure 2.4 - July time series of WRF output data for the 4 km (red trace) and 1.33 km (blue trace) domains at all Wasatch Front NAA METAR sites.

Table 2.1 - Statistical performance metrics for the NAA and N. Wasatch Front METAR sites. Benchmarks for simple and complex terrain are included after the corresponding statistic. Modeled values above established benchmarks are indicated by red font.

Table 2.2 - RMSE and bias for RH, 2-m temperature, 10-m wind speed, and 10-m wind direction at four UDAQ sites in the NAA. Values above established benchmarks are indicated by red font.

2.5. Vertical profiles and mixing layer height

Figure 2.5 - Average hourly ceilometer MLX at the Hawthorne (HW) DAQ monitoring station (2019-2022) for the month of July. 2020 data is included with a filled circle due to possible impacts from the COVID-19 shutdown. Average hourly PBLH for the nearest gridcell to HW (black stars) is included for comparison.

Figure 2.6 - Sounding-derived PBLH for daytime (12z) and nighttime (00z) (x markers) and the coincident WRF-PBLH at KSLC (circle markers). The right figure includes the sounding data and the PBLH anomaly (WRF- KSLC sounding observations) as black dots.

2.6 Spectral and surface observation nudging

Figure 2.7 - Observational nudging test. Obs nudging (red trace) vs benchmark WRF simulation (blue trace) for METAR sites in NAA.

3.Conclusions and future work

Appendix

Glossary of terms:

Table A1 - Vertical layer depths and heights used in WRF modeling

Table A2 - List of variables altered in the geogrid files.

Table A3 - Additional WRF output variables and their description

Figure A1 - 12 km domain spatial surface analysis for the modeling episode for 2m temperature, wind speed, mixing ratio, and wind direction.

Figure A2 - 12 km WRF and PRISM estimated precipitation totals for June 15-30th.

Figure A3 - 12 km anomaly precipitation for June 15-30th and the month of July.

Figure A4 - 4 km WRF and PRISM precipitation for June 15-30th.

Figure A5 - 4 km precipitation totals for July 2017.

Figure A6 - Lightning detected during the daytime (left panel) and nighttime (right panel) for the month of July, 2017.

Summary

The Northern Wasatch Front of Utah was bumped to moderate nonattainment of the 2015 ozone standard on November 7th, 2022.[1] The Utah Division of Air Quality (UDAQ) used a chemical transport model, CAMx (Comprehensive Air Quality Model with Extensions) to evaluate emission reductions and controls. Meteorological inputs for CAMx were generated using the weather research and forecasting model (WRF) version 4.2. This report includes specific model domains, simulation settings, and information on initialization/boundary condition datasets, as well as a model performance evaluation (MPE) for WRF. The WRF model performance evaluation was conducted primarily on the 4 and 1.33 km domains using the EPA-developed Atmospheric Model Evaluation Tool (AMET), and Python scripts for the entire simulation period of June 14th to August 2nd, 2017.

[1] EPA, 2022. Determinations of Attainment by the Attainment Date, Extensions of the Attainment Date, and Reclassification of Areas Classified as Marginal for the 2015 Ozone National Ambient Air Quality Standards. 87 FR 60897

1. WRF

The Weather Research and Forecasting Advanced Research model (WRF-ARW) version 4.2[2] was used to generate meteorological inputs for the selected chemical transport model, CAMx (Comprehensive Air quality Model with extensions). WRF has been used successfully for previous modeling efforts in Utah, including the PM2.5 State Implementation Plan (SIP). WRF has been used on a regional and national scale for ozone modeling efforts, including attainment demonstrations. Version 4.2 of WRF was the most updated release that worked within the demonstration timeline, and was selected in order to leverage the new terrain-following hybrid vertical coordinate system which should improve performance over complex terrain in this region.

The WRF simulation period, June 14th, 2017 at 12:00:00 UTC to August 2nd, 2017 at 00:00:00 UTC, was selected to include ozone exceedances in the summer of 2017 with adequate spin-up for photochemical modeling. This period excludes ozone exceedances that occurred in August, which were determined to be heavily influenced by regional wildfire emissions. In this document, the modeling episode refers to data from June 15th, 2017 at 00:00:00 UTC to August 1st, 2017 at 00:00:00 UTC unless otherwise noted.

1.1 WRF platform and preprocessor characteristics

[2] Skamarock, W. C., Klemp, J. B., Dudhia, J., Gill, D. O., Liu, Z., Berner, J., … Huang, X. -yu. (2019). A Description of the Advanced Research WRF Model Version 4 (No. NCAR/TN-556+STR). doi:10.5065/1dfh-6p97

Figure 1.1 - Extent of the 12, 4, and 1.33 km WRF modeling domains

1.1.1 Modeling domains and vertical layers

The WRF model domains were keyed to the EPA-developed US1 12 km domain, and chosen to accommodate the desired extent of the CAMx domains. The three one-way nested WRF domains were set to the Lambert Conformal Conic projection with horizontal resolution of 12, 4, and 1.33 km, respectively (Figure 1.1). Grids were offset from the default reference coordinates using ref_x = 222.5 and ref_y = 153.5. Each domain has 44 vertical levels which are identical to the EPA ORD 108km hemispheric modeling configuration. This configuration includes decreased layer thickness (higher vertical resolution) near the surface. Table 1.1 includes an abbreviated representation of approximate layer heights above ground level (AGL) and layer thickness. A more detailed table can be found in appendix Table A1 .

WRF layer	Eta	press. (mb)	height AGL(m)	depth (m)	altitude (m)
45	0	5000	17556	1177	18,844
41	0.0816	12752	13481	818	14,769
34	0.269	30555	8519	611	9,808
25	0.595	61487	3744	415	5,032
18	0.837	84544	1332	203	2,620
11	0.949	95174	397	70	1,685
7	0.978	97920	169	39	1,457
5	0.988	98813	96	29	1,384
3	0.995	99487	41	22	1,329
2	0.998	99763	19	19	1,307
1	1.000	100000	0	0	1,288

Table 1.1 - Summary of vertical levels and level thicknesses

1.1.2 Atmospheric data selection (IC/BC)

This modeling demonstration leveraged the National Center for Environmental Protection North American Mesoscale (NAM) 12 km analysis dataset (ds609)[3] to provide initial conditions (IC) for all modeling domains, and continually provide boundary conditions

[3] National Centers for Environmental Prediction/National Weather Service/NOAA/U.S. Department of Commerce. 2015, updated daily. NCEP North American Mesoscale (NAM) 12 km Analysis. Research Data Archive at the National Center for Atmospheric Research, Computational and Information Systems Laboratory. https://doi.org/10.5065/G4RC-1N91.

(BC) to the outermost (12 km) domain. Analysis data was integrated at 6-hour time intervals throughout the duration of the simulation.

1.1.3 Geographic data selection

WRF V4.2 defaults to MODIS-derived geographic/land use datasets, of which the 21-category (MODIS + Lakes) were used for this modeling effort. A 30-arcsecond resolution was used for the 12-km outermost domain, with 15-arcsecond resolution used for the 4 and 1.33km domains. Although the USGS geographic datasets have a slightly better representation of the Great Salt Lake (GSL), the urban land fraction was not well represented and all default WRF land use datasets were created over 10 years ago. For the episode modeled here, MODIS data was selected and modified to more accurately reflect changes to the GSL (described in the following section).

1.1.4 Adjustments to the Great Salt Lake Extent

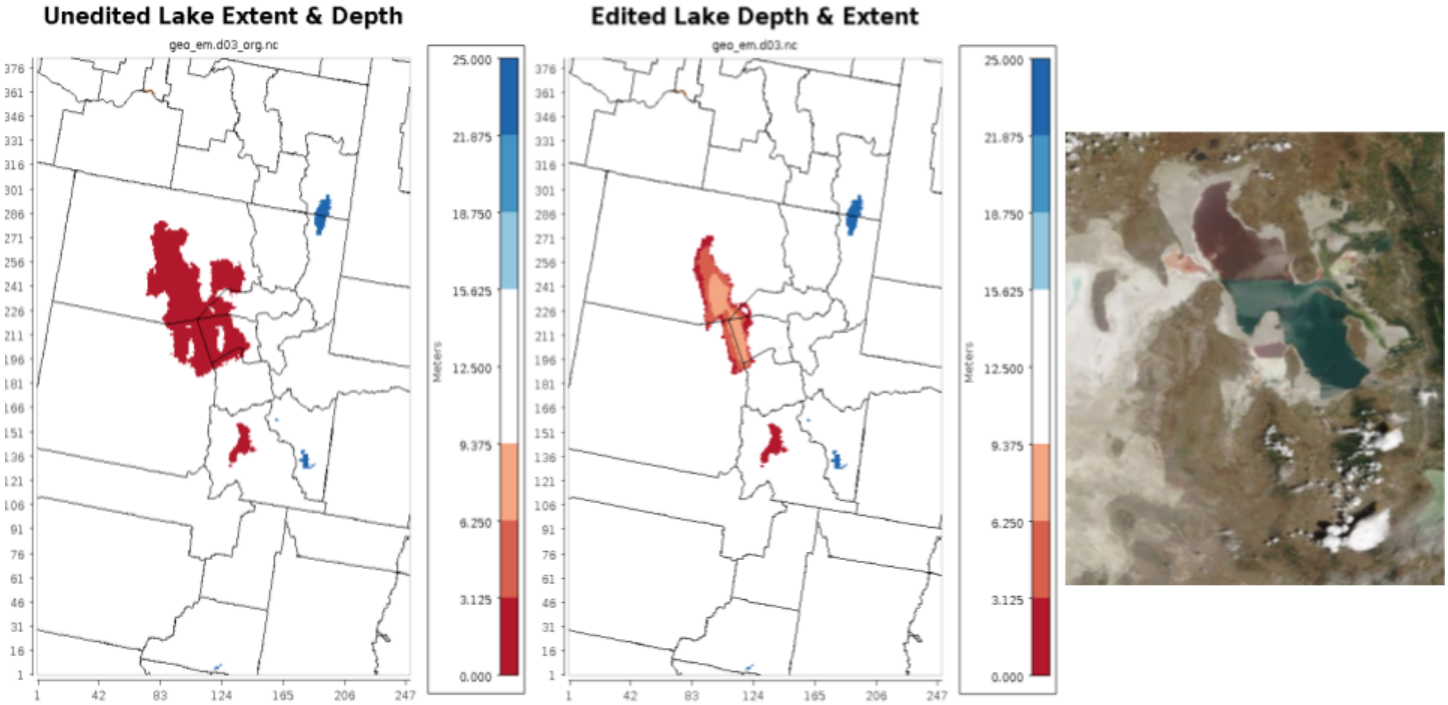

Figure 1.2 - Great Salt Lake extent and depth before (left panel) and after (middle panel) adjusting the WRF geogrid files to reflect the GSL levels in mid-July of 2017 (right panel).

The default MODIS data does not accurately reflect the extent of the lake in July of 2017 (Figure 1.2). The lake extent was decreased following the method detailed by Mallia et al[4]

[4]Mallia, D. V. (2018). *Simulating High Impact Wildfire and Wind-Blown Dust Events Using Improved Atmospheric Modeling Methods*. Ph.D. Dissertation. University of Utah. Available at: https://collections.lib.utah.edu/ark:/87278/s6pp4hgm

which adjusts the lake boundary and depth using bathymetry and lake buoy observational data. After adjusting the true lake extent, areas that were incorrectly classified as "lake" were adjusted to reflect the characteristics of unvegetated salt flats. Table A2 in the Appendix includes the initial and final values of all altered land use variables.

One impact from the lake adjustment is the exposure of more playa, a surface with a higher albedo than water, proximate to the Wasatch Front urban corridor. Observations along the GSL boundary suggest that polluted air masses from the SLV experience higher ozone production as they are transported over the higher-albedo lake playa surface. Land-lake breezes can result in a return of that polluted air mass, leading to higher concentrations of ozone in the SLV[5].

1.1.5 Additional Pre-Processor Selections

The WPS utility, avg_tsfc.exe, was used to adjust the temperature of the GSL. The generated average daily surface temperature was generally higher than the default values.

1.1.6 WRF Parameters Summary Table

Table 1.2 summarizes the grid information and land use data selected for this demonstration.

Parameter	D01	D02	D03
Resolution	12 km	4 km	1.33 km
Grid size (x,y)	(287, 299)	(291, 291)	(249, 381)
Vertical levels	44	44	44
Vertical coordinates	Hybrid vertical coordinates	Hybrid vertical coordinates	Hybrid vertical coordinates
IC/BC	NAM 12 km	NAM 12 km/D01	NAM 12 km/D02
Land Use Dataset	MODIS + lakes 30 arc-second	MODIS + lakes 15 arc-second	MODIS + lakes 15 arc-second

[5] Horel, J. (2015) *The Great Salt Lake Ozone Study Final Report*. Available at: https://documents.deq.utah.gov/air-quality/planning/technical-analysis/research/northern-utah-airpollution/gsl-ozone/DAQ-2017-014353.PDF

Table 1.2 - WRF model grid configurations, land use, and initial/boundary conditions.

1.2 WRF Model Configuration

The initial physics options used for this WRF modeling episode were selected based on standard selections used by the EPA and similar modeling efforts completed for other Western States[6]. Results from a subset of sensitivity tests, including surface observational nudging, are summarized in Section 2.5.1.

1.2.1 Model run length and outputs

The model episode (06/15/2017 - 08/02/2017) was run in 5.5 day chunks starting at 12z. The first 12-hours of simulation were considered spin-up time and discarded from further analysis. Two or more 5.5-day periods were run simultaneously to take advantage of multiple computation nodes. WRF data was output every hour and combined into 12-hour files (two per day).

1.2.2 Physics options

Table 1.3 includes the relevant physics options used for the WRF modeling episode. Cumulus parameterization was used for the 12 and 4 km domains to yield daily precipitation/cloud cover that had better agreement with the PRISM data product (Section 2.4). No additional lightning convection parameterization was readily available for the simulation time period, and was not included in the WRF simulation.

Table 1.3 - Physics options for WRF namelist

Parameter	D01 (12 km)	D02 (4 km)	D03 (1.33 km)
Microphysics	Thompson graupel scheme (2-moment)	Thompson graupel scheme (2-moment)	Thompson graupel scheme (2-moment)
Radiation	RRTMG	RRTMG	RRTMG

[6] Ramboll. (2019) *WRF Meteorological Modeling to Support Denver 2020 and 2023 Ozone Attainment Demonstration Modeling - Draft Report*. Available at: https://raqc.egnyte.com/dl/VAyfCiMspB/WRF_Denver_2016_2019-08v3.pdf_

Land Surface Model	Noah LSM	Noah LSM	Noah LSM
Planetary Boundary Layer	MYNN Level 2.5	MYNN Level 2.5	MYNN Level 2.5
Cumulus Parameterization	Multi-scale Kain-Fritsch	Multi-scale Kain-Fritsch	none

1.2.3 Dynamics options

As mentioned previously, the hybrid vertical coordinate system was used in this simulation (hybrid_opt = 2). The horizontal Smagorinsky first order closure (km_opt =4) and 6th-order numerical diffusion (diff_6th_opt = 2) were selected for the diffusion options. Raleigh dampening (damp_opt = 3, dampening coefficient of 0.2) was used for the upper level dampening flag.

1.2.4 Data assimilation & Nudging

Grid nudging above the planetary boundary layer (PBL) was included for the 12 km domain following the default WRF namelist FDDA (Four Dimensional Data Assimilation) options. Additional nudging of the 4 and 1.33 km domains using surface observations was tested but did not appear to improve performance with the selected nudging coefficients and is an area for future work (Section 2.7).

1.2.5 Additional output variables

CAMx requires additional output variables from the WRF simulation that are not generally included in the output files. The variables in Table A3 were added using the iofields list option. Table A3 includes the additional output variables and their description.

2. Model Performance Evaluation

The EPA-developed Atmospheric Model Evaluation Tool (AMET)[7] Version 1.4 was primarily used to evaluate the performance of WRF. AMET was chosen for its ease of use and automation of statistical performance metrics including: mean absolute error (MAE), mean bias (MB), index of agreement (IOA), root mean square error (RMSE), normalized mean bias (NMB), and the anomaly correlation (AC). Additional temperature, relative humidity, wind performance, and surface radiation evaluation was conducted at UDAQ stations within the NAA using Python Version 3.9.

Temperature, mixing ratio, wind direction, and wind speed at the 2 and 10-meter level were chosen for statistical analysis due to the completeness of observational datasets (described below). A direct comparison of the planetary boundary layer height (PBLH) during the modeling episode, using rawinsonde data, is further supported by a qualitative PBLH analysis using ceilometer data only available after the modeling episode. A comparative spatial analysis was performed for modeled precipitation, and more in-depth comparisons of modeled vs. observed surface radiation aid evaluation of non-precipitating cloud cover.

2.1 Observational Datasets

AMET includes a direct data download from the NCEP Meteorological Assimilation Data Ingest System (MADIS) for a variety of observational types (surface, vertical profiles, radiation measurements), and networks. Unfortunately, a glitch in data upload between the MesoWest/Synoptic Data network and MADIS resulted in all stations missing data from 03:00 UTC through 06:00 UTC. Though only ~25% of the data is missing (and generally still considered "OK" by data completeness standards), the fact that all of the data is missing during local nighttime hours can skew the statistical results of AMET analysis. For this reason, METAR sites (uploaded to MADIS through a different network) were selected for analysis using AMET tools. Although there are fewer METAR sites, there are six sites along the Wasatch Front and four within the nonattainment area (Figure 2.1). Salt Lake City International airport (KSLC) is the closest METAR site to the controlling ozone monitor evaluated in the SIP. For further analysis of UDAQ monitoring stations, meteorological

[7] Gilliam RC, Appel W, and Philips S (2005). The Atmospheric Evaluation Tool (AMET): Meteorology Module, presented at the 4th Annual CMAS Conference, September 26–28, 2005, http://www.cmascenter.org/conference/2005/abstracts/6_1.pdf.

variables were downloaded directly from the EPA-supported Air Quality System (AQS).[8] Radiation data from UDOT stations was downloaded via the Mesowest Network.[9]

Daily and monthly precipitation totals were evaluated using the PRISM dataset. Because WRF was run in 5.5-day segments, daily precipitation accumulation of WRF was compared to the daily PRISM data product. These daily values were summed over the domain in order to compare both the June 15-30th and July time periods. Data of lightning detected from the Lightning Imaging Sensor (LIS[10]) on the International Space Station was checked in order to support the lack of deep convection in the Northern Wasatch Front to investigate the importance (or not) of an additional lightning dataset product.

Figure 2.1 - METAR sites along the Wasatch Front. KOGD, KHIF, KSLC, and KU42 are a part of the ozone NAA.

[8] US Environmental Protection Agency. Air Quality System API [internet database] available via https://aqs.epa.gov/data/api/metaData/. Accessed August 10, 2022.
[9] Horel, J., et al. (2002). MESOWEST: COOPERATIVE MESONETS IN THE WESTERN UNITED STATES, Bulletin of the American Meteorological Society, 83(2), 211-226. Retrieved Jan 13, 2023, from https://journals.ametsoc.org/view/journals/bams/83/2/1520-0477_2002_083_0211_mcmitw_2_3_co_2.xml
[10] Blakeslee, Richard J.. 2020. Quality Controlled Lightning Imaging Sensor (LIS) on International Space Station (ISS) Science Data LIS ISS Space Time Domain Search. Dataset available online from the NASA Global Hydrology Resource Center DAAC, Huntsville, Alabama, U.S.A. DOI: http://dx.doi.org/10.5067/LIS/ISSLIS/DATA108

2.2 Spatial Surface Analysis (12 km)

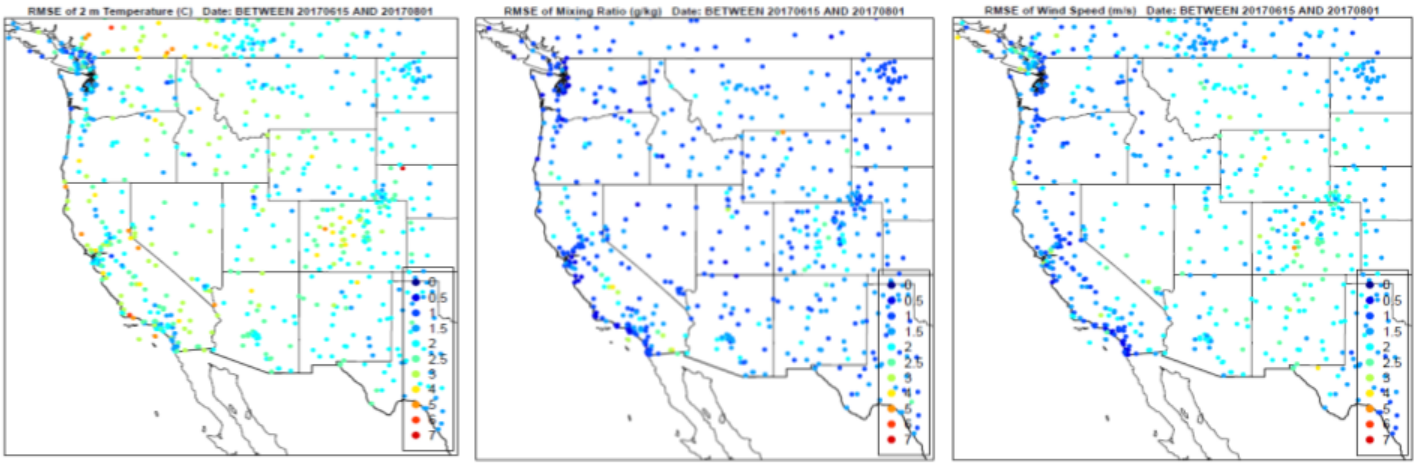

Figure 2.2 - RMSE of 2m temperature, mixing ratio, and wind speed for the 12 km domain (D01).

Although the majority of model performance was conducted for the 4 and 1.33 km domains, precipitation and performance of METAR sites within the 12 km domain is also included in this report. Figure 2.2 includes the RMSE for temperature, mixing ratio, and wind speed throughout the 12km domain for the modeled episode (2017/06/15 to 2017/08/01). Error is generally within the established benchmarks (listed in Table 2.1) for these variables throughout the domain. The RMSE of wind direction (included in Figure A1) has poor performance and is an area for future improvement.

Section 2.3 PRISM analysis

To evaluate how well WRF simulated precipitation during the episode, data from the Parameter-elevation Relationships on Independent Slopes Model (PRISM) product generated by Oregon State University [11] was used as a comparison dataset. Although PRISM is a observation-based estimate of precipitation, there are many challenges in producing the dataset, especially over regions with few precipitation stations or radar coverage[12]. Daily WRF vs PRISM performance is highly variable, and this MPE focused primarily on monthly precipitation averages. This analysis uses the 4 km resolution PRISM dataset for all WRF domain comparisons.

[11] PRISM Climate Group, Oregon State University, https://prism.oregonstate.edu, data created 21 Oct 2019, accessed 21 September 2021.
[12] Daly, C., Challenges in Observation-Based Mapping of Daily Precipitation across the Conterminous United States, Journal of Atmospheric and Oceanic Technology, vol. 38, no. 11, pp. 1979–1992, 2021. doi:10.1175/JTECH-D-21-0054.1.

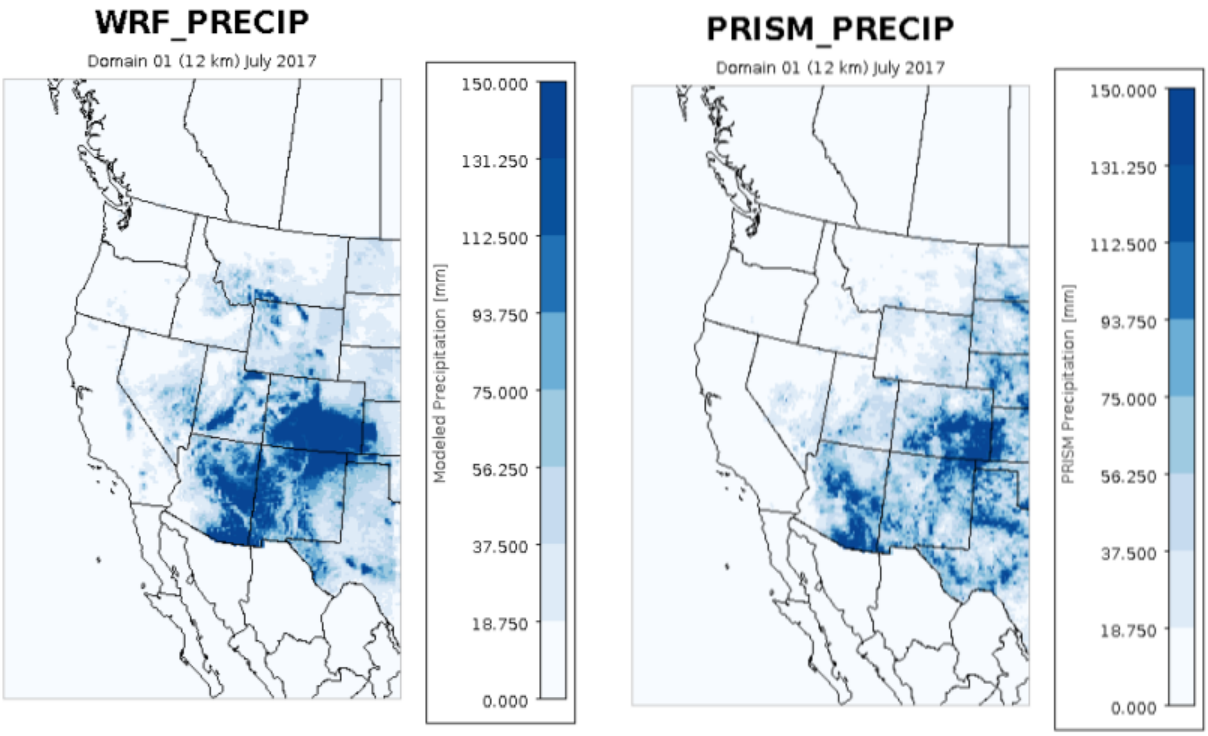

Figure 2.3 - July total WRF and PRISM estimated precipitation (mm) over the 12 km domain

Figure 2.3 includes the 12 km WRF and PRISM outputs for the month of July. Figures (including anomaly plots) for all domains and time periods not pictured in this section are included in Figures A2, A3, A4, and A5. Overall, WRF generally overestimates precipitation compared to PRISM over the entire 12 km domain, especially in mountainous regions in Northern Utah and Colorado. Precipitation totals in Western Utah/Eastern Nevada were low for both June and July.

The June (15-30th) and July precipitation anomalies for the 4 km domain (Figure 2.4) offer more insight into WRF performance over our modeling region of interest. PRISM estimated almost no precipitation in the state of Utah during the June episode dates, and WRF generally overestimated precipitation by about 3 mm (~ 0.1 inches). Distribution of precipitation events in June is also fairly consistent between WRF and PRISM [Figure A4]. WRF precipitation anomalies in the NAA range between -12 mm to 25 mm (-0.5 to 0.9 inches) for the month of July, and precipitation patterns are simulated well for Utah and the western part of the 4 km domain [Figure A5].

Anomaly plots of the 4 km (Figure 2.4) and 1.33 km domains (Figure 2.5) also support that model agreement over the NAA is good, and that very little precipitation occurred within the NAA during the simulation period. These long-term averages don't easily depict specific thunderstorms or how well WRF simulates non-precipitating clouds which can

shade the region and reduce photochemistry. Section 2.4 includes more information about WRF surface radiation performance.

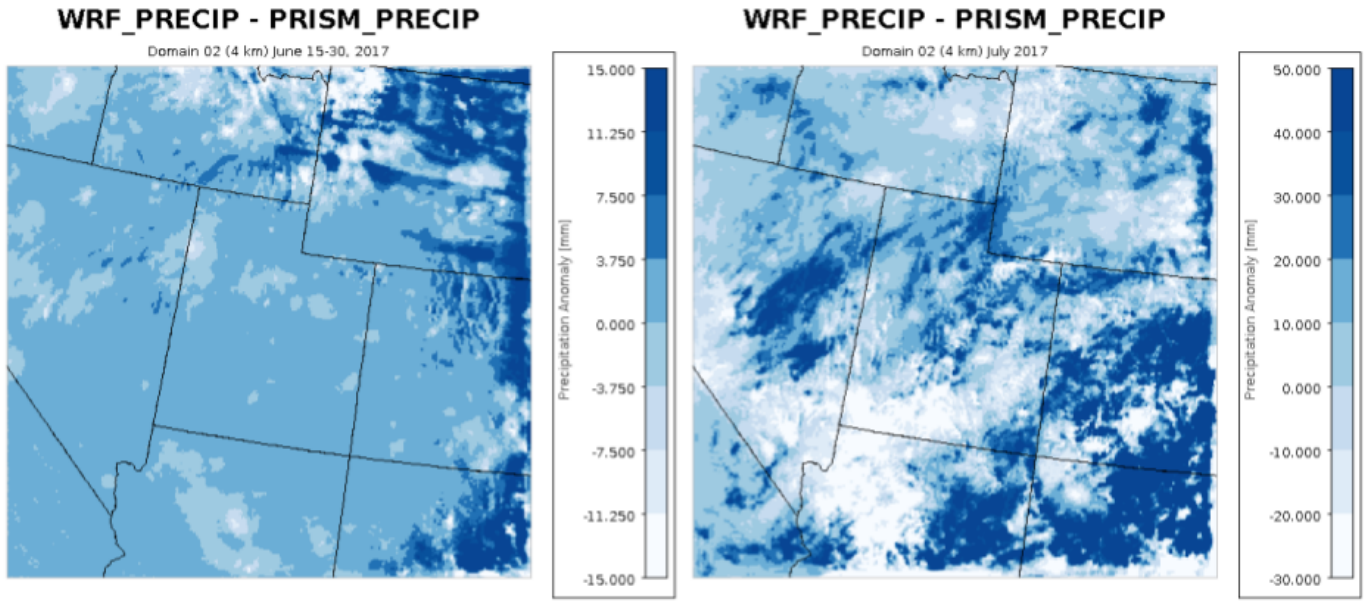

Figure 2.4 - 4 km precipitation anomaly plots (WRF-PRISM) for June 15-30, 2017 (left) and July 2017 (right).

An additional check of domain-wide convection was performed using the LIS dataset. Although this dataset has coarse temporal and spatial coverage, it also suggests that very few lightning flashes were detected in July of 2017, which is consistent with lack of heavy convection (Figure A6).

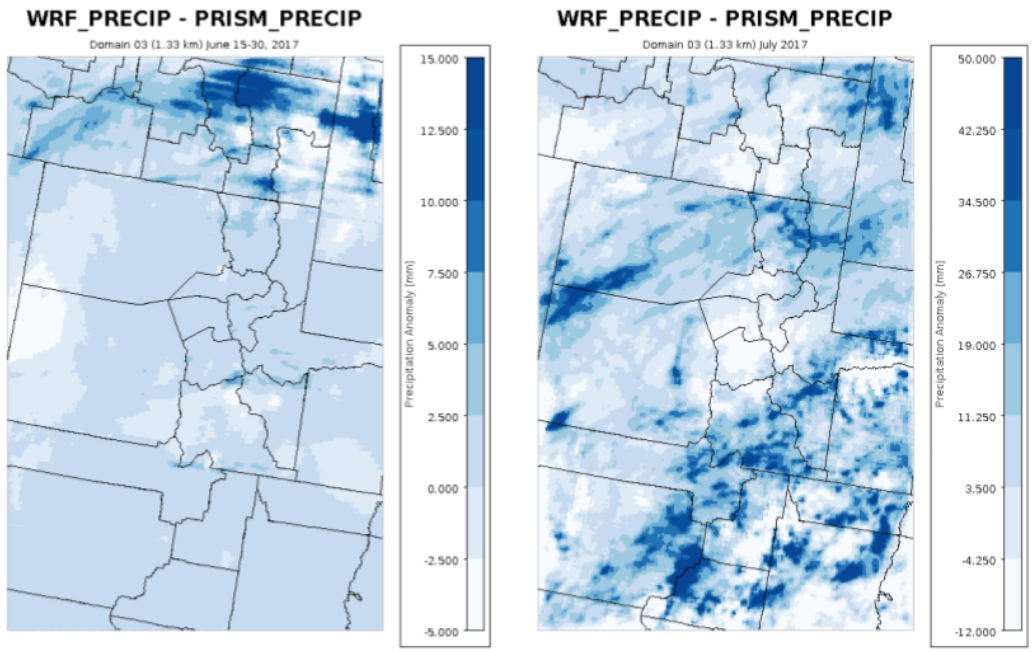

Figure 2.5 - Precipitation anomaly plots (WRF-PRISM) for the 1.33 km modeling domain.

2.4 Surface radiation and cloud cover

CAMx modeling using these WRF outputs has days during the episode when modeled ozone concentrations are higher than observations, especially during a frontal passage towards the end of July. To investigate WRF radiation performance, met stations in the Mesowest network were filtered to find observations that were as close as possible to three UDAQ sites (Figure A7). Two sites, those within 3 km of the Hawthorne (HW) and Bountiful (BV) UDAQ stations, are from the Mesowest network, and are labeled by their orientation to the UDAQ stations for reference (BV_e and HW_w). A third set of observations from the now-retired UDAQ Syracuse station (SR) are also included in this analysis. Observations at the top of the hour are compared to WRF outputs for the same grid cell in the 1.33 km modeling domain.

On average, WRF overestimates the maximum daily radiation value by approximately 40 W/m^2 at SR, 90 W/m^2 at BV_e, and 120 W/m^2 at HW_w. Some of this discrepancy is likely due to differences in instrumentation and siting. HW_w is located at a busy highway interchange, while BV_e is on the slope of the Wasatch bench.

Four time segments that include periods of reduced CAMx ozone performance are included in Figure 2.6. The three sites show how variable cloud cover is across the 1.33 km domain. For instance, on July 7th, observations from HW_e and BV_e indicate some light cloud cover, while SR is more impacted throughout the day. WRF does not capture cloud coverage at any site on July 14th, which is reflected in higher modeled ozone from CAMx

than observations at BV. Similarly, on July 23rd, modeled ozone is higher than observations at both BV and HW sites.

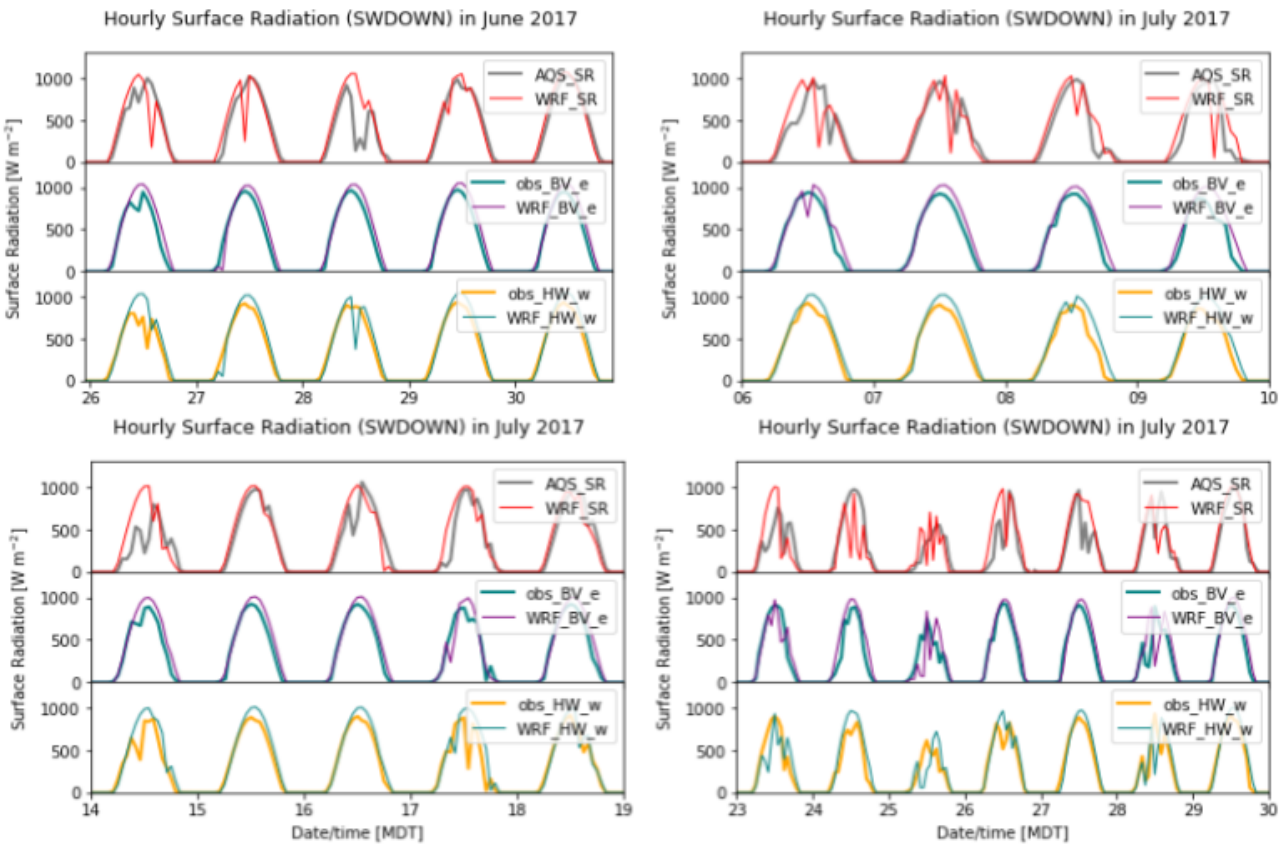

Figure 2.6 - Shortwave radiation observations (bold lines) and WRF outputs for select time periods during the modeling episode.

2.5 Time series analysis

Figure 2.7 includes mixing ratio, temperature, relative humidity, and station pressure of the grouped nonattainment area METAR sites for the modeling episode. Although the 12 km domain (D01, red line) performs better than the 4 km domain (D02, blue line) for mixing ratio, temperature, and relative humidity, the station pressure performance highlights the power of averaging over the domain. The 12 km pressure performed much worse due to the complex terrain of the Wasatch Front (including a large lake). Similarly, a higher-resolution domain should improve SMOKE emissions distribution and photochemical model performance despite the slightly higher biases in temperature and mixing ratio/relative humidity.

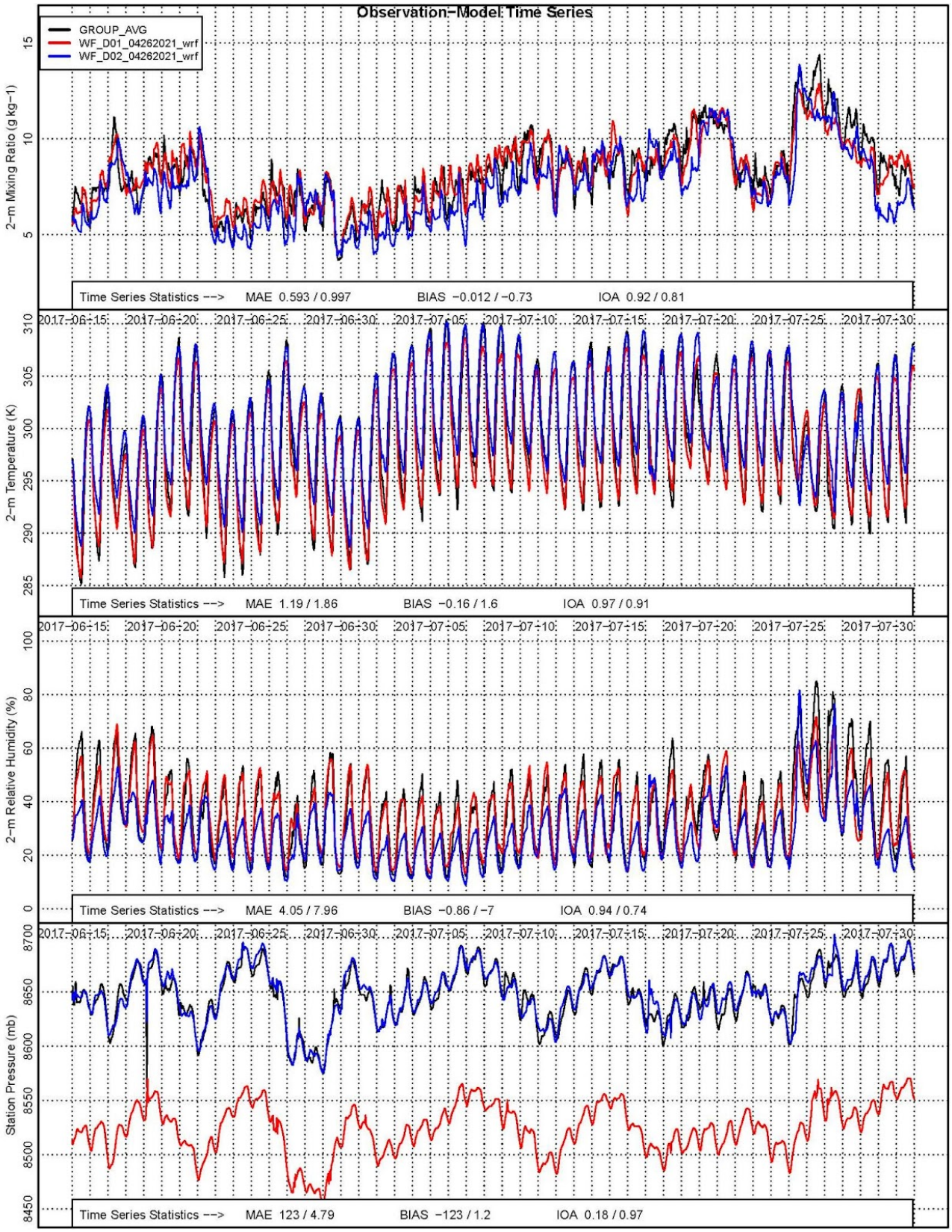

Figure 2.7 - Time series of WRF simulation for METAR sites within the NAA.

Figure 2.8 includes the 12 and 4 km domain information for the METAR site closest to the NAA controlling monitor, KSLC. The time series statistics are similar to the grouped sites, with WRF trending warmer at night and drier as the resolution increases. Wind direction (not shown) is similarly underestimated at all domain resolutions.

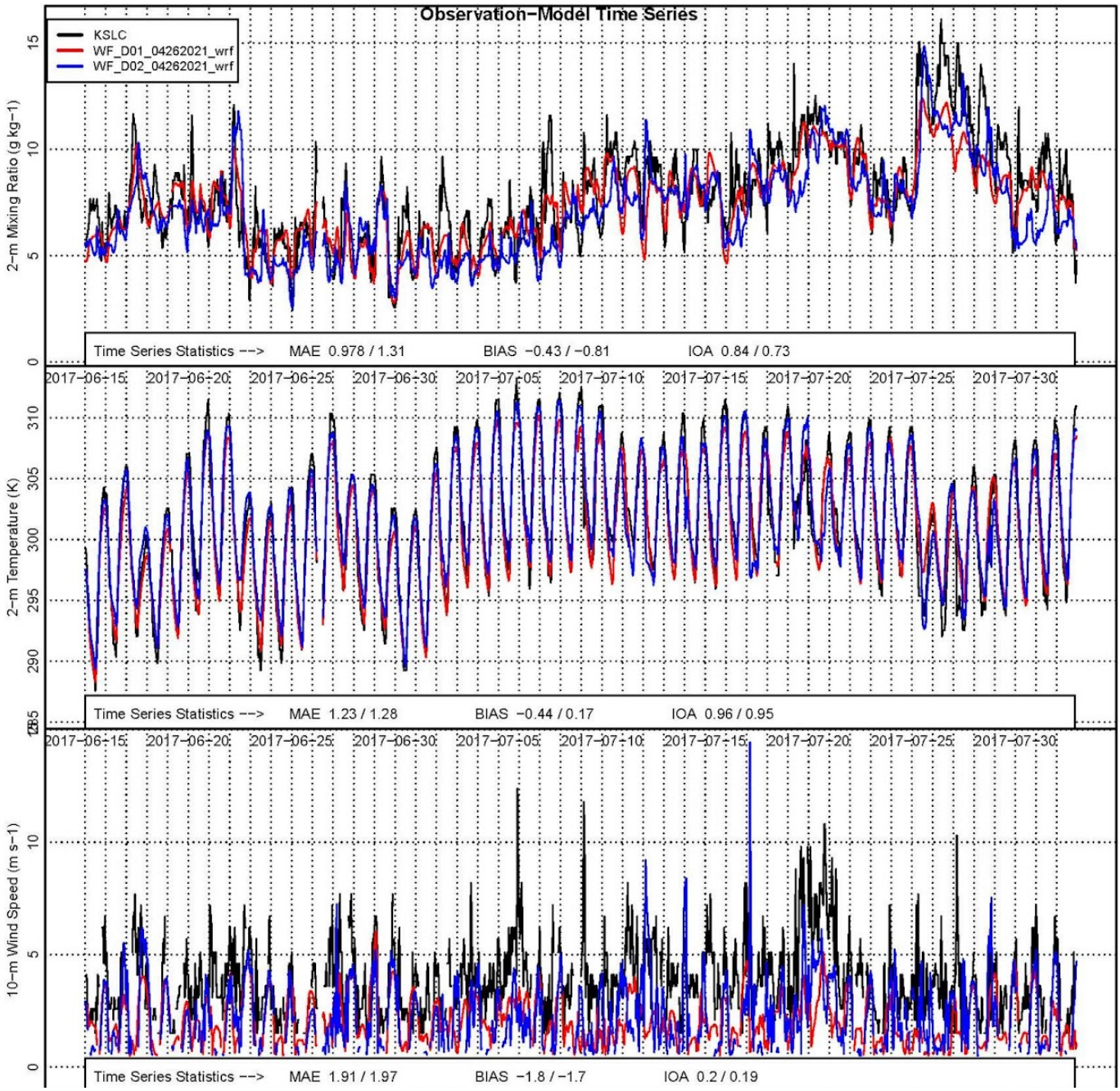

Figure 2.8 - Time series of modeled vs observations at KSLC for D01 and D02

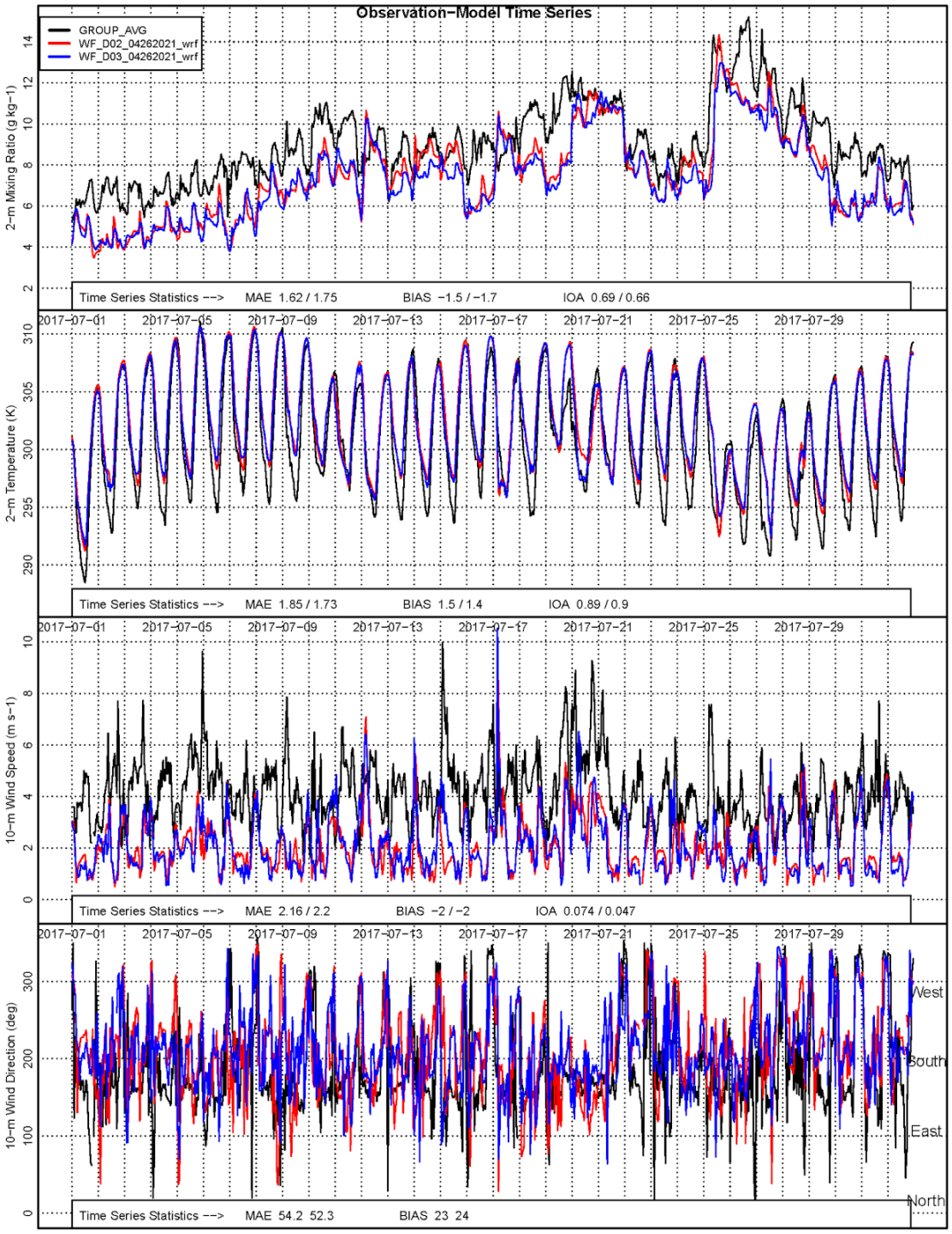

Figure 2.9 - July time series of WRF output data for the 4 km (red trace) and 1.33 km (blue trace) domains at all Wasatch Front NAA METAR sites.

The model performance of selected state variables generally decreased with increasing model domain resolution. Some of this error is due to grid-cell averaging for the lower resolution domains. The decrease in performance between the 4 and 1.33 km domains

(Figure 2.9) is generally minimal (< 10%). WRF has a warm temperature bias, especially during the evening hours, lower wind speeds, and drier conditions than observations.

Table 2.1 summarizes the RMSE, MB, and IoA of the 2-meter mixing ratio and temperature, as well as the 10-m wind speed and direction for the METAR sites within the NAA (n=4) and the Northern Wasatch Front (n=6).

Meteorological performance benchmarks were pulled from the UNC/ENVIRON study (2011)[13] which summarizes the simple performance benchmarks identified by Emery (2001) [14] and those adapted for more complex terrain by Kemball-Cook (2005)[15]. By these metrics, observations from the Wasatch Front and NAA METAR sites agree well with model outputs for both 2-m temperature and mixing ratio. Wind speed and wind direction, however, perform worse than established benchmarks and have poor correlation. WRF is known to underestimate surface winds, especially in areas with lower wind speeds[16], and there is no complex terrain benchmark for wind direction bias. The Wasatch Front also experiences a variety of wind disturbance patterns at the surface, including drainage flows from the many surrounding canyons and breezes from the Great Salt Lake[17] [18].

---

[13] UNC and ENVIRON, 2014. 3SAQS WRF 2011 Meteorological Model Application/Evaluation. University of North Carolina, Chapel Hill, NC. ENVIRON International Corporation, Novato, CA. July 2014. Available at: http://views.cira.colostate.edu/documents/projects/tsdw/Meetings/Technical_Workshop_20130529/3SAQS_WRF_2011_Modeling_Protocol_Draft_3.pdf

[14] Emery, C., E. Tai, and G. Yarwood, 2001. "Enhanced Meteorological Modeling and Performance Evaluation for Two Texas Ozone Episodes." Prepared for the Texas Natural Resource Conservation Commission, prepared by ENVIRON International Corporation, Novato, CA. 31-August. http://www.tceq.texas.gov/assets/public/implementation/air/am/contracts/reports/mm/EnhancedMetModelingAndPerformanceEvaluation.pdf

[15] Kemball-Cook, S., Y. Jia, C. Emery and R. Morris. 2005. "Alaska MM5 Modeling for the 2002 Annual Period to Support Visibility Modeling" Prepared for Western Regional Air Partnership (WRAP). Prepared by Environ International Corporation. September. http://pah.cert.ucr.edu/aqm/308/docs/alaska/Alaska_MM5_DraftReport_Sept05.pdf

[16] Blaylock, B. K., Horel, J. D., & Crosman, E. T. (2017). Impact of Lake Breezes on Summer Ozone Concentrations in the Salt Lake Valley, Journal of Applied Meteorology and Climatology, 56(2), 353-370. Retrieved Nov 10, 2022, from https://journals.ametsoc.org/view/journals/apme/56/2/jamc-d-16-0216.1.xml

[17] Baasandorj, M., Hoch, S. W., Bares, R., Lin, J. C., Brown, S. S., Millet, D. B., Martin, R., Kelly, K., Zarzana, K. J., Whiteman, C. D., Dube, W. P., Tonnesen, G., Jaramillo, I. C., and Sohl, J.: Coupling between Chemical and Meteorological Processes under Persistent Cold-Air Pool Conditions: Evolution of Wintertime PM2.5 Pollution Events and N2O5 Observations in Utah's Salt Lake Valley, Environ. Sci. Technol., 51, 5941–5950, https://doi.org/10.1021/acs.est.6b06603, 2017.

[18] Crosman, E.T., Horel, J.D. Sea and Lake Breezes: A Review of Numerical Studies. Boundary-Layer Meteorol 137, 1–29 (2010). https://doi.org/10.1007/s10546-010-9517-9

Table 2.1 - Statistical performance metrics for the NAA and N. Wasatch Front METAR sites. Benchmarks for simple and complex terrain are included after the corresponding statistic. Modeled values above established benchmarks are indicated by red font.

NAA Sites	RMSE (D01/D02/D03)	Benchmark Simple, Complex	Bias (D01/D02/D03)	Benchmark Simple, Complex	IoA (D01/D02/D03)
2-m Mixing ratio (g/kg)	1.1, 1.8, 1.9	≤ ± 2.0, **NA**	-0.67, **-1.4, -1.5**	≤ ± 1.0, **NA**	0.85, 0.71, 0.68
2-m Temperature (K)	1.3, 2.3, 2.2	≤ 2.0, **≤ 3.5**	0.24, 1.6, 1.5	≤ ±0.5, **≤ ±2.0**	0.97, 0.91, 0.91
10-m Wind Speed (m/s)	2, 2.5, 2.5	≤ 2.0, **≤ 2.5**	**-1.6, -1.9, -1.9**	≤ ±0.5, **≤ ±1.5**	0.2, 0.095, 0.074
	MAE (D01/D02/D03)	**Benchmark Simple, Complex**	**Bias (D01/D02/D03)**	**Benchmark Simple, Complex**	
10-m Wind Dir (degrees)	55, 55, 54	≤ 30, **≤ 55**	-2.6, **21, 19**	≤ ±10, **NA**	
N. WaFr Sites	**RMSE (D01/D02/D03)**	**Benchmark Simple, Complex**	**Bias (D01/D02/D03)**	**Benchmark Simple, Complex**	**IoA (D01/D02/D03)**
2-m Mixing ratio (g/kg)	0.8,1.2,1.1	≤ ± 2.0, **NA**	0.056, -0.64, -0.52	≤ ± 1.0, **NA**	0.91, 0.82, 0.83
2 -m Temperature (Kelvin)	1.3, 2.2, 2.2	≤ 2.0, **≤ 3.5**	-0.07, 1.5, 1.4	≤ ±0.5, **≤ ±2.0**	0.97, 0.91, 0.92
10-m Wind Speed (m/s)	1.8, 1.4, 2.3	≤ 2.0, **≤ 2.5**	-1.4, **-1.7, -1.8**	≤ ±0.5, **≤ ±1.5**	0.2, 0.91, 0.92
	MAE (D01/D02/D03)	**Benchmark Simple, Complex**	**Bias (D01/D02/D03)**	**Benchmark Simple, Complex**	
10-m Wind Dir (degrees)	**59**, 48, 51	≤ 30, **≤ 55**	**-14**, 9.6, **18**	≤ ±10, **NA**	

Table 2.2 looks at similar statistics for relative humidity, temperature, wind speed, and wind direction for the UDAQ monitoring stations in the NAA (n=4). WRF compares less favorably to the UDAQ observations for 2-m temperature and wind direction, but most values are still within established benchmarks. Performance metrics for modeled wind speed at UDAQ sites are better than those for the NAA METAR sites, but that might be due to differences in sighting of these stations (i.e nearby trees or taller buildings). Unlike the METAR sites, WRF wind speeds are generally higher than observations for the UDAQ sites. There are no established benchmarks for relative humidity, but the trend of WRF being drier and hotter than observations is consistent.

Table 2.2 - RMSE and bias for RH, 2-m temperature, 10-m wind speed, and MAE for 10-m wind direction at four UDAQ sites in the NAA. Values above established benchmarks are indicated by red font.

NAA Sites	RMSE (D01/D02/D03)	Benchmark Simple, Complex	Bias (D01/D02/D03)	Benchmark Simple, Complex
2-m RH %	5.7, 11.2, 12.5	**NA, NA**	-2.2, -6.4, -8.2	**NA, NA**
2-m Temperature (K)	1.7, 2.7, 2.9	≤ 2.0, **≤ 3.5**	0.2, 1.6, **2.1**	≤ ±0.5, **≤ ±2.0**
10-m Wind Speed (m/s)	1.6, 1.7, 1.4	≤ 2.0, **≤ 2.5**	0.9, 0.7, 0.3	≤ ±0.5, **≤ ±1.5**
	MAE (D01/D02/D03)	**Benchmark Simple, Complex**	**Bias (D01/D02/D03)**	**Benchmark Simple, Complex**
10-m Wind Dir (degrees)	**82**, **94**, **107**	≤ 30, **≤ 55**	**-19.3**, **-27.1**, -9.5	≤ ±10, **NA**

2.6 Vertical profiles and mixing layer height

The DAQ monitoring network does not have ceilometer data for the summer of 2017, but Figure 3 includes a comparative analysis of average hourly ceilometer mixing layer height (MLX) and the WRF planetary boundary layer height (PBLH) at the Hawthorne monitoring location for recent years of available data. The WRF PBLH is generally higher than the ceilometer data, especially during the afternoon and early evening hours.

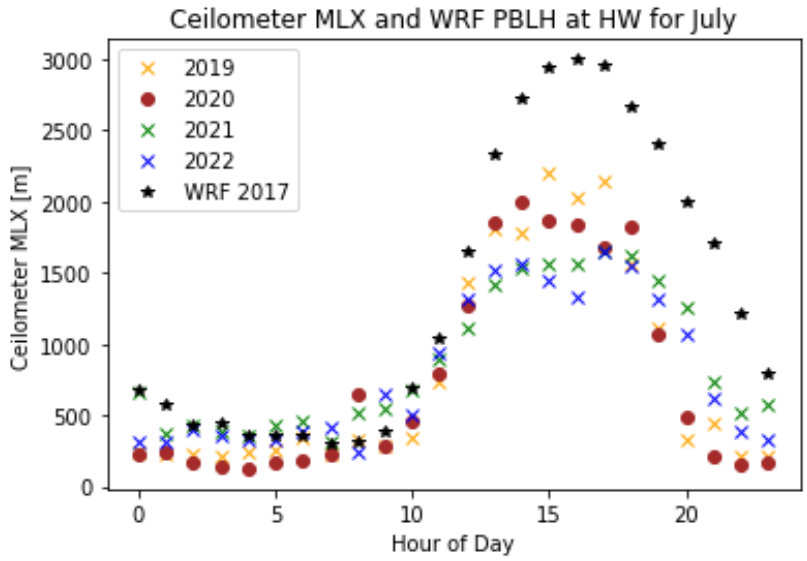

Figure 3 - Average hourly ceilometer MLX at the Hawthorne (HW) DAQ monitoring station (2019-2022) for the month of July. 2020 data is included with a filled circle due to possible impacts from the COVID-19 shutdown. Average hourly PBLH for the nearest gridcell to HW (black stars) is included for comparison.

To better compare the WRF outputs to observations, rawinsonde data from KSLC was used to calculate an observed PBLH value for July of 2017. WRF PBLH data from the KSLC gridcell was pulled for both the 00 UTC (6 pm local time) and 12 UTC (6 am local time). Though not perfect, this gives a more useful comparison of PBLH than the standard AMET vertical profile analysis. Figure 3.1 includes the sounding-derived PBHL for the daytime and nighttime during the month of July. The left plot includes both WRF and sounding-derived data, while the right includes the PBLH anomaly (WRF - sounding). WRF generally overestimates the PBLH during the 6 am "daytime" sounding, which yields a thicker PBLH than observations suggest.

A thicker PBLH from WRF could impact nighttime surface ozone titration in CAMx. Further exploration into this possible phenomenon revealed that, although this WRF simulation uses the MYNN PBL physics option (Table 1.3), the wrfcamx preprocessor recalculates the PBLH, resulting in a thinner nighttime PBLH for the photochemical modeling.

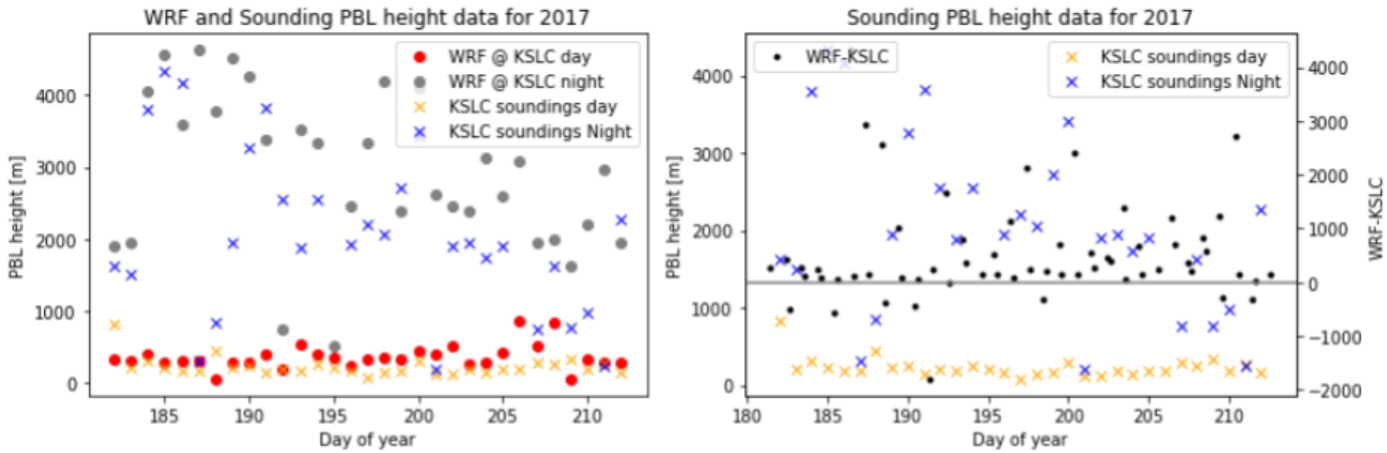

Figure 3.1 - Sounding-derived PBLH for daytime (12z) and nighttime (00z) (x markers) and the coincident WRF-PBLH at KSLC (circle markers). The right figure includes the sounding data and the PBLH anomaly (WRF- KSLC sounding observations) as black dots.

2.7 Spectral and surface observation nudging

Initial tests for both spectral nudging and surface observation nudging showed decreased performance for this simulation episode. Spectral nudging introduced temperature and mixing ratio anomalies at surface sites. Observational nudging was performed on the 4 and 1.33 km domains (D02 and D03) for temperature, moisture, and wind. Both temperature and moisture had higher MAE and biases in the nudging scenario, but there was some improvement in wind speed (Figure 3.2). Due to time constraints, simulations with different nudging coefficients were not tested and are an area of future work.

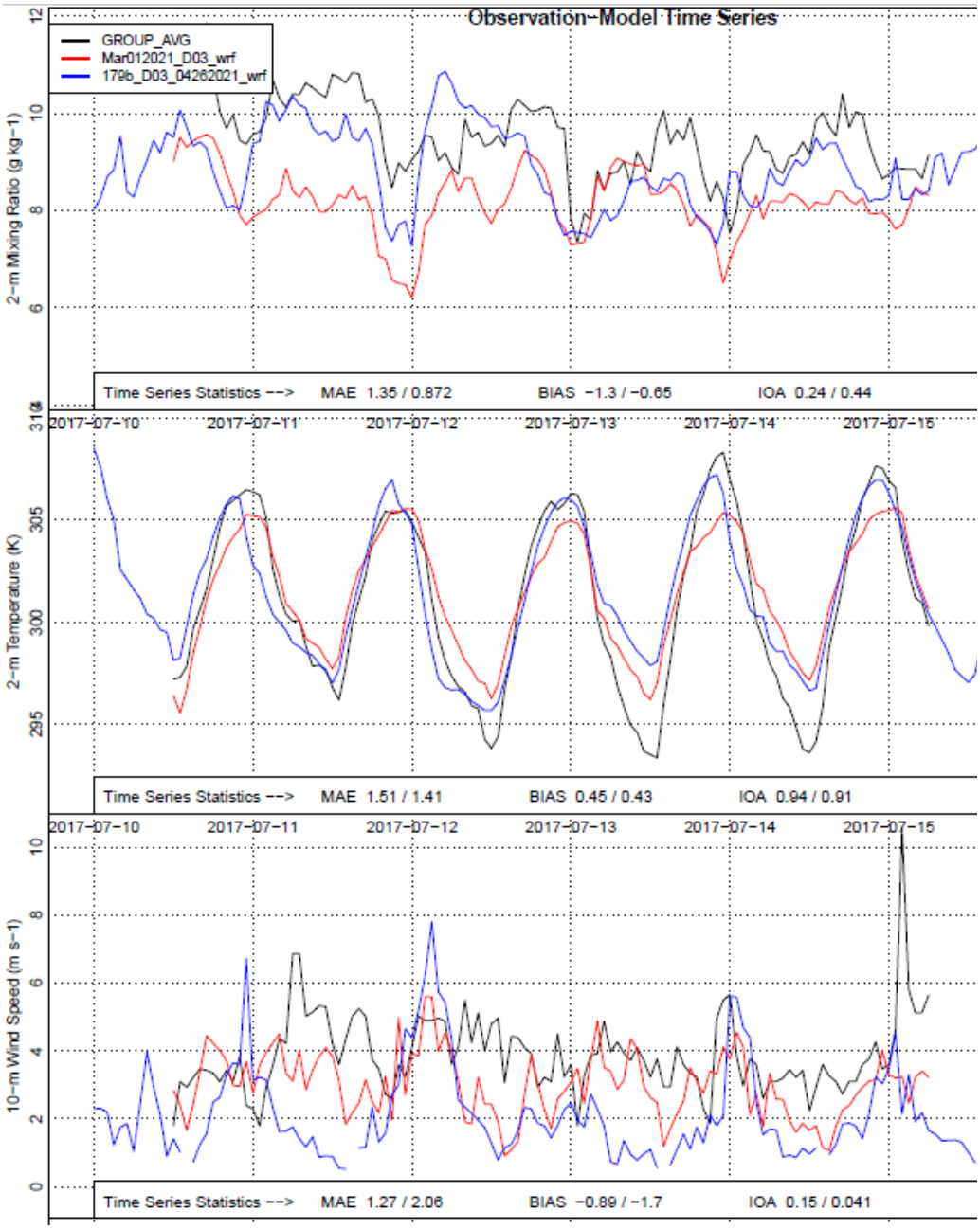

Figure 3.2 - Observational nudging test. Obs nudging (red trace) vs benchmark WRF simulation (blue trace) for METAR sites in NAA.

3.Conclusions and future work

WRF does an adequate job of simulating 2-m temperature trends at all domain resolutions. WRF temperature bias is higher than observations, especially during the nighttime hours, and does slightly exceed established benchmarks for temperature bias in the 1.33 km domain at the subset of NAA UDAQ stations. For moisture variables, WRF has a dry bias that increases with increasing domain resolution, but the model performs well averaged over the Northern Wasatch Front. Correlation between modeled and observed moisture and temperature variables is also very good for most domains.

WRF wind direction and wind speed performance are areas for future improvement. Poor performance is likely due, in part, to the complex terrain and variety of factors that influence surface wind flows. These include land-lake breeze from the GSL and air exchange from the multitude of nearby canyons. Modeled 10-m wind speeds are generally lower than observations at both the NAA and Northern Wasatch Front METAR sites, but higher than observations at UDAQ sites. The wind speed bias is also outside of the established benchmark for complex terrain, though variable between the METAR and UDAQ sites. WRF MAE of wind direction is barely within established benchmarks for the METAR sites, but exceeds the complex terrain benchmark at UDAQ stations. All of these shortfalls are consistent with the low surface winds observed during our modeling episode.

Precipitation modeled by WRF is generally higher than that of the PRISM dataset, but performance within the NAA for the time period of interest shows precipitation is underestimated by 0.5-1” for the month of July. Future modeling years may be characterized by more deep convection, which could require a lightning assimilation tool to improve model performance. Analysis of surface radiation observations indicate spotty cloud coverage over the WRF domain that is often underestimated by WRF at certain stations, which can overproduce ozone in the CAMx simulation.

The limitations in WRF performance could lead to underestimated ozone levels in the chemical transport model, though underperformance in some areas could be counteractive. For instance, the overestimated PBL could yield erroneously diluted ozone precursor emissions and underestimated surface ozone, but underestimated wind speeds could concentrate precursors emissions, somewhat negating dilution through vertical dispersion. The hotter and drier modeled conditions could yield more ozone production in CAMx, but incorrectly modeled cloud cover could reduce (or increase) ozone production.

WRF simulations for future SIP demonstrations are already underway. WRF v4.4 shows improved performance for temperature, wind speed, wind direction and moisture using the same input data and namelist options. Tests to improve the PBLH using different boundary layer schemes (YSU, MYJ) have improved nighttime PBLH, but these schemes have poor temperature and moisture performance. Time constraints prevented further observational nudging tests, but may be included in future SIP demonstrations once the CAMx platform has been established.

Appendix

Glossary of terms:

AC - Anomaly Correlation

AGL - Above Ground Level

AQS - Air Quality System

BC - Boundary Conditions

AMET - Atmospheric Model Evaluation Tool

CAMx - Comprehensive Air Quality Model with Extensions

EPA - Environmental Protection Agency

FDDA - Four Dimensional Data Assimilation

GSL - Great Salt Lake

IC - Initial Conditions

IOA - Index of Agreement

KSLC - Salt Lake City international airport

LIS - Lightning Imaging sensor

MADIS - Meteorological Assimilation Data Ingest System

MAE - Mean Absolute Error

MB - Mean Bias

MLX - Mixing Layer Height

MODIS - Moderate Resolution Imaging Spectroradiometer

MPE - Model Performance Evaluation

NAA - Non Attainment Area

NCEP - National Centers for Environmental Protection

NMB - Normalized Mean Bias

ORD - Office of Research and Development

PBL - Planetary Boundary Layer

PBLH - Planetary Boundary Layer Height

PRISM - Parameter elevation Regression on Independent Slopes Model

RMSE - Root mean square error

UDAQ - Utah Division of Air Quality

UTC - Universal Time Coordinated (also Coordinated Universal Time)

WRF - Weather research and forecasting model

WRF-AWR - Weather Research and Forecasting Advanced Research model

Table A1 - Vertical layer depths and heights used in WRF modeling

WRF Eta Levels					
WRF layer	Eta	Pressure (mb)	Height AGL (m)	Depth (m)	Altitude (m)
45	0	5000	17556	1177	18,844
44	0.0186	6767	16379	1062	17,667
43	0.0386	8667	15317	958	16,605
42	0.0596	10662	14359	878	15,647
41	0.0816	12752	13481	818	14,769
40	0.1047	14947	12662	769	13,950
39	0.1289	17246	11893	730	13,181
38	0.1543	19659	11163	699	12,451
37	0.181	22195	10464	669	11,752
36	0.2089	24846	9795	649	11,083
35	0.2383	27639	9146	626	10,434
34	0.269	30555	8519	611	9,808
33	0.3013	33624	7908	597	9,196
32	0.3352	36844	7311	585	8,599
31	0.371	40226	6727	573	8,015
30	0.408	43770	6154	537	7,442
29	0.445	47313	5617	506	6,905
28	0.483	50857	5111	479	6,399
27	0.520	54400	4632	455	5,920
26	0.557	57944	4177	433	5,465
25	0.595	61487	3744	415	5,032
24	0.632	65040	3329	396	4,617
23	0.669	68584	2933	380	4,221
22	0.707	72127	2553	365	3,841
21	0.744	75671	2188	336	3,476
20	0.780	79053	1853	282	3,141
19	0.810	81988	1571	239	2,859
18	0.837	84544	1332	203	2,620
17	0.861	86767	1128	173	2,417
16	0.881	88695	956	148	2,244
15	0.899	90377	807	127	2,095
14	0.914	91840	680	109	1,968
13	0.928	93113	571	94	1,859
12	0.939	94215	477	81	1,765
11	0.949	95174	397	70	1,685
10	0.958	96010	327	61	1,615
9	0.966	96742	266	52	1,554
8	0.972	97369	214	45	1,502
7	0.978	97920	169	39	1,457
6	0.983	98395	130	34	1,418
5	0.988	98813	96	29	1,384
4	0.991	99174	67	25	1,355
3	0.995	99487	41	22	1,329
2	0.998	99763	19	19	1,307
1	1.000	100000	0	0	1,288

Table A2 - List of variables altered in the geo_em WPS files.

Variable	Old Value & Category	New Value & Category
LAKE_DEPTH	3 meters for entire lake	Calculated from bathymetry (0.2 - 8.2 m)
LANDMASK	0 (denotes lake)	1 (denotes land)
SCT_DOM	14 (denotes lake)	11 (silty clay)
SCB_DOM	14 (denotes lake)	8 (silty clay loam)
SANDFRAC	0 (denotes lake)	0.33 (fraction of sand)
CLAYFRAC	0 (denotes lake)	0.34 (fraction of clay)
SOILTEMP	0 (denotes lake)	290.80 K
LU_INDEX	21 (denotes lake)	16 (barren/sparsely vegetated)
3-D Variables		
ALBEDO12M	8, 8, 8 (Values for J, J, A)	34, 35, 33 (Values for J, J, A)
LANDUSEF	21 (denotes lake)	16 (barren/sparsely vegetated)
SOILCTOP	14 (denotes lake)	11 (silty clay)
SOILCBOT	14 (denotes lake)	8 (silty clay loam)

Table A3 - Additional WRF output variables and their description

Variable	Description
LANDUSEF	Landuse fraction by category
RA	Aerodynamic resistance
RS	Surface resistance
PRATEC	Precip rate from cumulus scheme
GSW	Net short wave flux at ground surface
ZNT	Time-varying roughness length
RMOL	1./Monin Ob. length
MOL	T* in similarity theory
CLDFRA_DP	Deep convective cloud fraction from KF
CLDFRA_SH	Shallow convective cloud fraction from KF
QC_CU	Cloud water mixing ratio from a CU scheme
QI_CU	Ice water mixing ratio from a CU scheme
UER_KF	Updraft entrainment rate from KF
UDR_KF	Updraft detrainment rate from KF
DER_KF	Downdraft entrainment rate from KF
DDR_KF	Downdraft detrainment rate from KF
TIMEC_KF	Convective time scale from MSKF
PREC_ACC	Cumulative precipitation

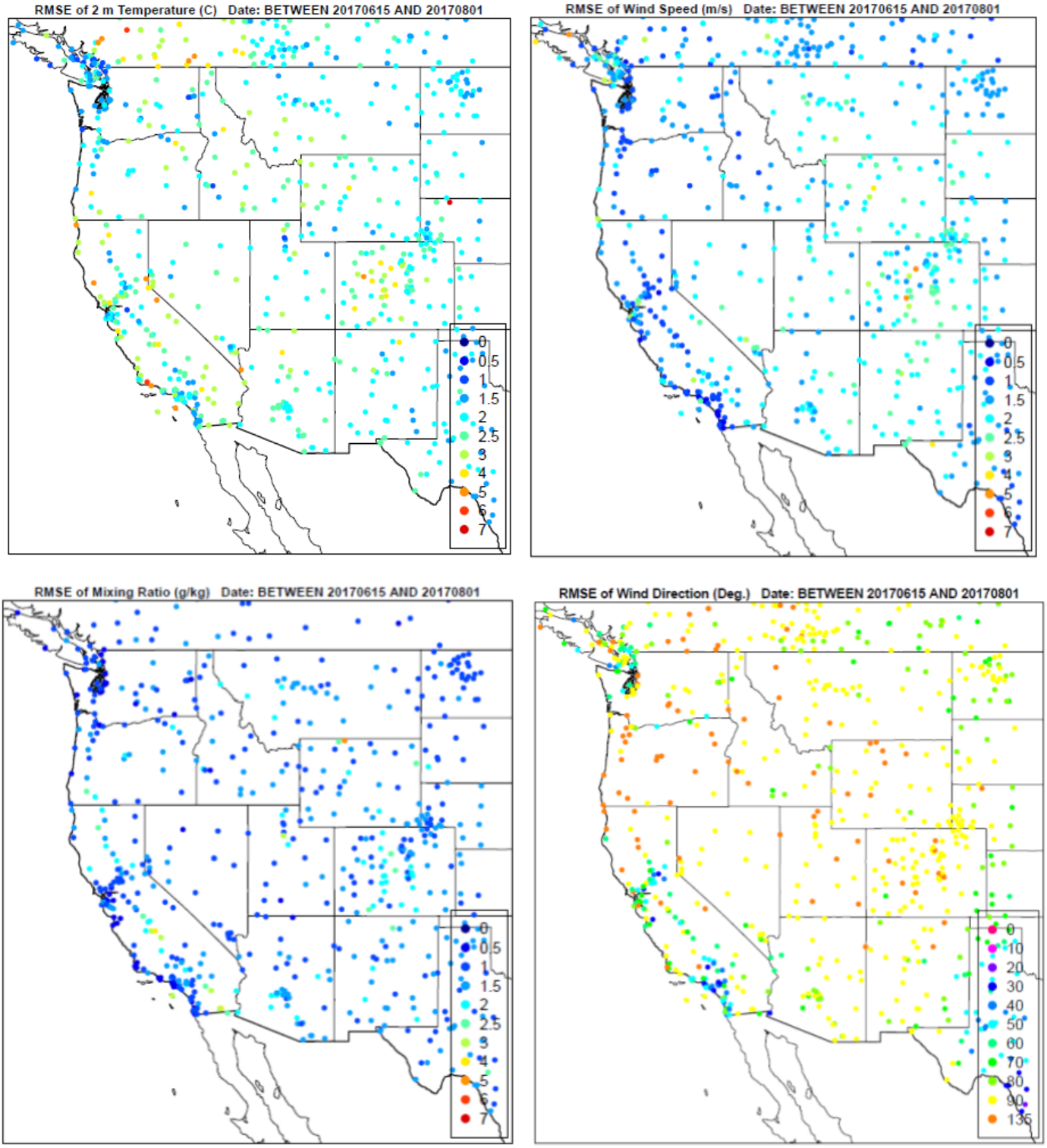

Figure A1 - 12 km domain spatial surface analysis for the modeling episode for 2m temperature, wind speed, mixing ratio, and wind direction.

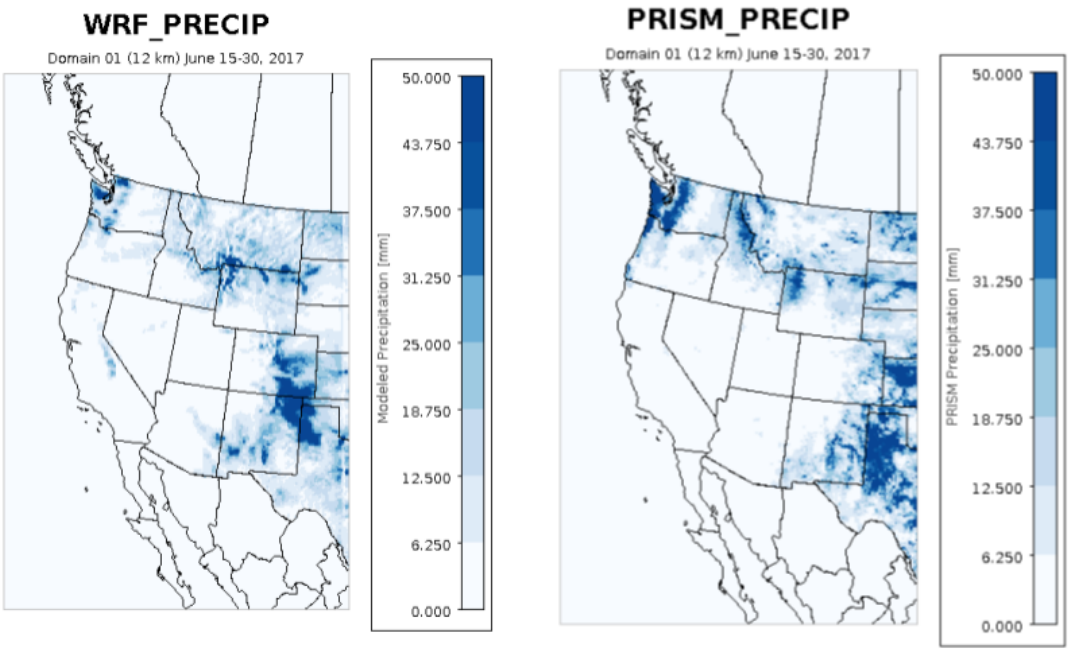

Figure A2 - 12 km WRF and PRISM estimated precipitation totals for June 15-30th.

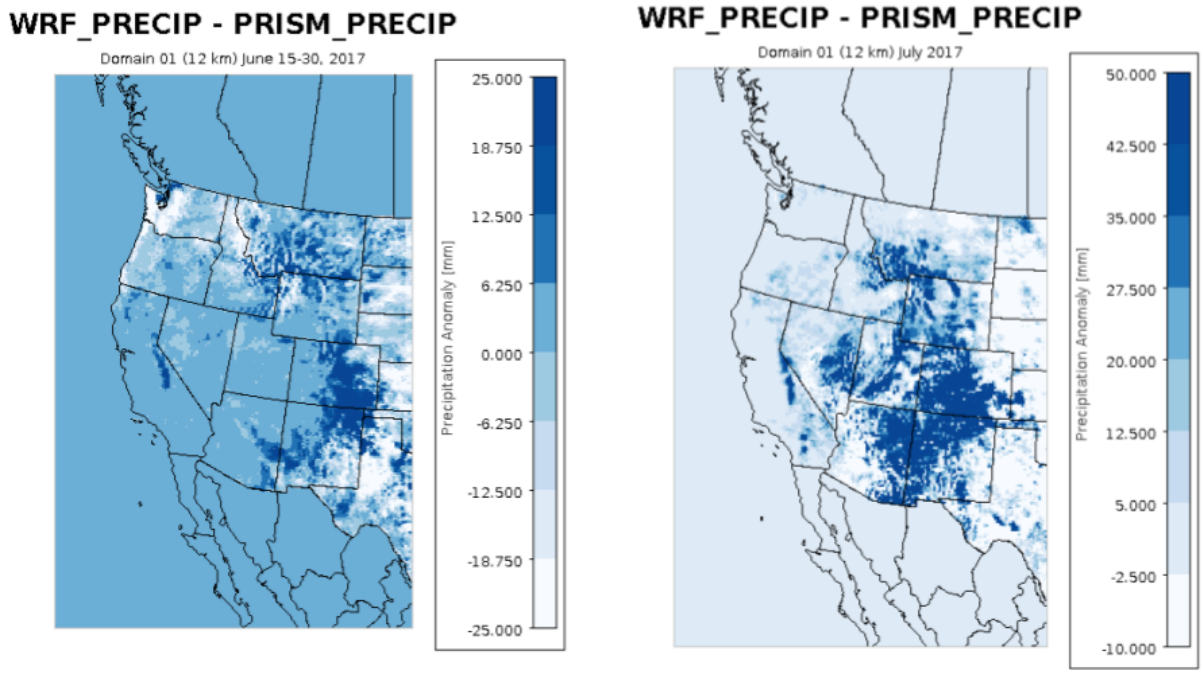

Figure A3 - 12 km anomaly precipitation for June 15-30th and the month of July.

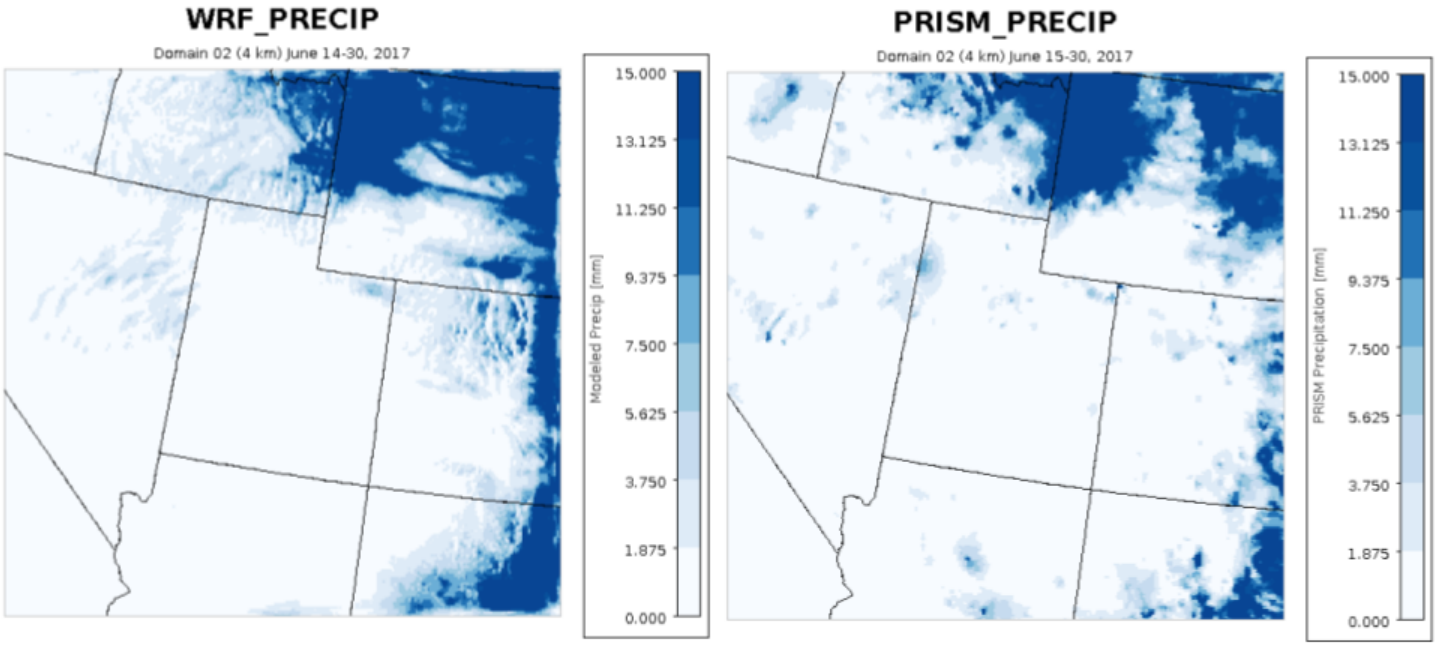

Figure A4 - 4 km WRF and PRISM precipitation for June 15-30th.

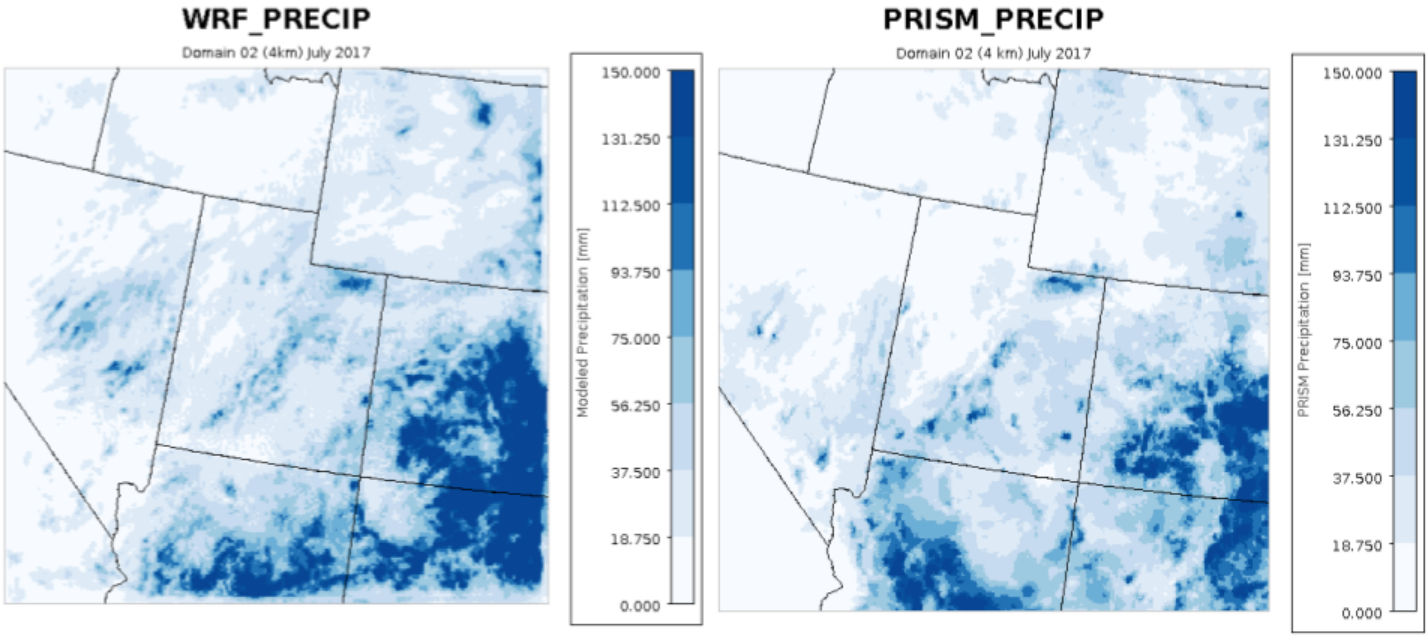

Figure A5 - 4 km WRF and PRISM precipitation totals for July 2017.

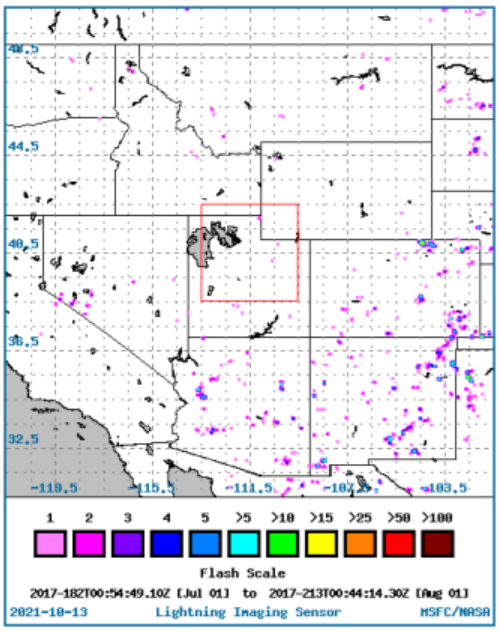

Number of orbits searched: 461
Number of orbits with flashes in the area of interest (red rectangle): 3
Number of flashes detected in the area of interest (red rectangle): 4
Total number of flashes in the image: 902

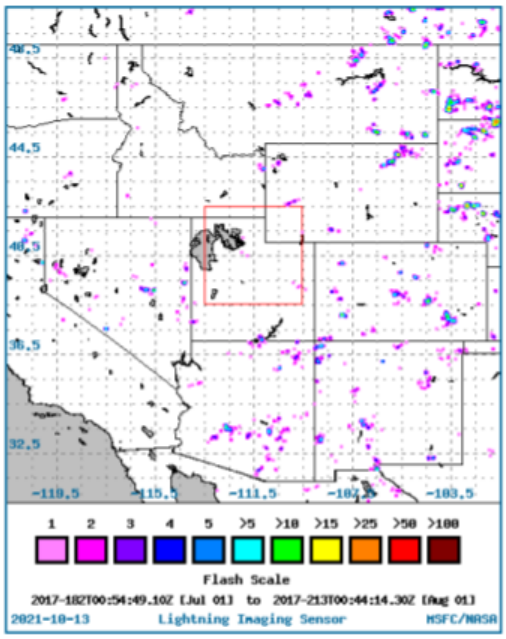

Number of orbits searched: 461
Number of orbits with flashes in the area of interest (red rectangle): 4
Number of flashes detected in the area of interest (red rectangle): 7
Total number of flashes in the image: 2090

Figure A6 - Lightning detected during the daytime (left panel) and nighttime (right panel) for the month of July, 2017.

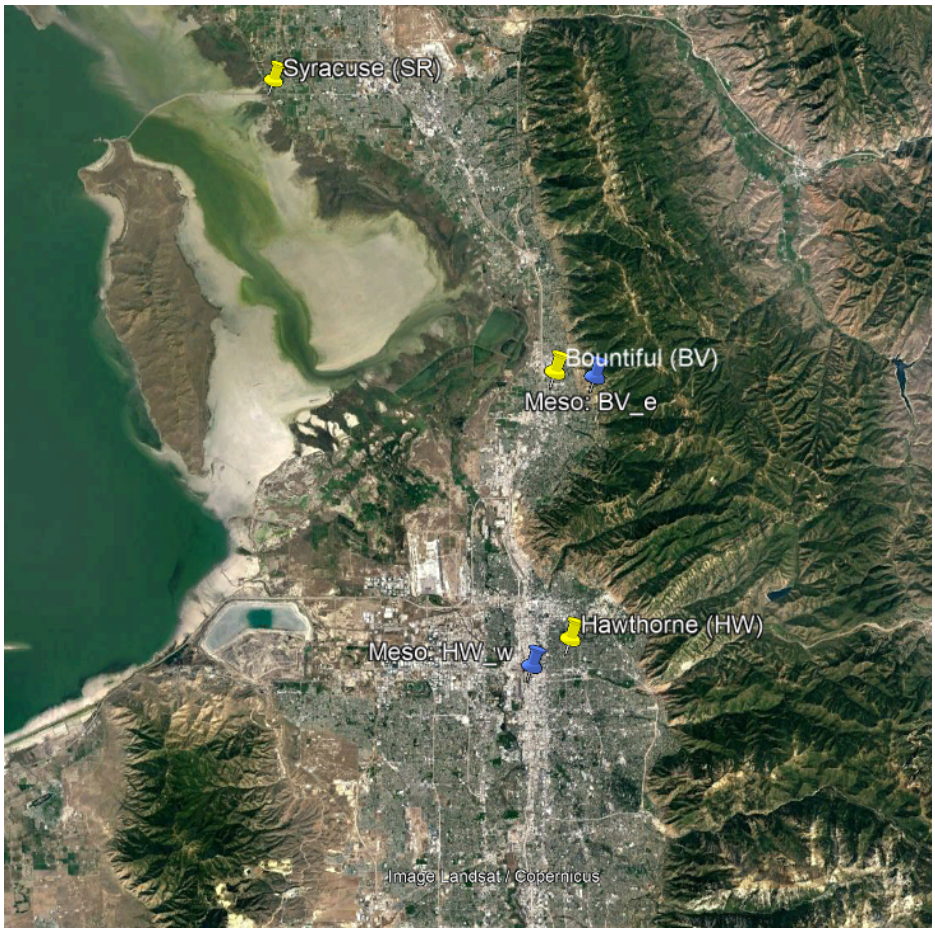

Figure A7 - Location of UDAQ monitors (yellow pins) and their orientation to Mesowest monitors (blue pins) used for surface radiation analysis.